RECONFIGURABLE INTELLIGENT SURFACE-AIDED NEAR-FIELD COMMUNICATIONS FOR 6G

Opportunities and Challenges

Xidong Mu, Jiaqi Xu, Yuanwei Liu, and Lajos Hanzo

Reconfigurable intelligent surface (RIS)-aided near-field communications are investigated. First, the necessity of investigating RIS-aided near-field communications and the advantages brought about by the unique spherical wave-based near-field propagation are discussed. Then, the family of patch array-based RISs and metasurface-based RISs is introduced along with respective near-field channel models. A pair of fundamental performance limits of RIS-aided near-field communications, namely, their power scaling law and effective degrees of freedom (EDOF), are analyzed for both patch array-based and metasurface-based RISs, which reveals the potential performance gains that can be achieved. Furthermore, associated near-field beam training and beamforming design issues are studied, where a two-stage hierarchical beam training approach and a low-complexity element-wise beamforming design are proposed for RIS-aided near-field communications. Finally, a suite of open research problems is highlighted for motivating future research.

Introduction

With the rapidly spreading rollout of the 5G wireless network across the globe, researchers have turned their attention to 6G concepts. One of the key objectives is to enhance the data rate, latency, and space–air–ground coverage and harness pervasive intelligence [1]. To fulfill these stringent requirements, transmission technologies have to be further enhanced, relying on the employment of extremely large multiple-input, multiple-output (MIMO) schemes, millimeter-wave (mm-wave)/terahertz (THz) bandwidths, and satellite communications, just to name a few directions [1]. Furthermore, hitherto unknown groundbreaking technologies should be conceived for revolutionizing the family of existing wireless technologies. Among these new technologies, RISs, having a massive number of low-cost electromagnetic (EM) reflection elements, constitute one of the most promising technologies for 6G. RISs can be deployed in wireless networks for beneficially ameliorating the signal propagation for much needed signal enhancement and interference mitigation [2]. More importantly, the near-passive full-duplex characteristics of RISs render them more attractive than active relaying technologies that have expensive power-hungry radio-frequency chains. Therefore, RIS-aided wireless communications pave the way for sustainable and ubiquitous 6G services.

Given the aforementioned benefits, extensive research efforts have been devoted to RIS-aided wireless communications, including but not limited to passive beamforming coefficient design, channel estimation,

and deployment location design [2]. However, the majority of existing investigations relied on the assumption of far-field propagation, where both the incident and refracted/reflected wireless signals exhibited a planar wavefront, as shown in Figure 1(a). By contrast, in RIS-aided near-field communications, the wavefront of wireless signals should be accurately characterized by the spherical wavefront, as in Figure 1(b).

From Planar Wave-Based Far-Field Propagation to Spherical Wave-Based Near-Field Propagation

Again, the signal propagation of RISs can be divided into near-field and far-field regions. One of the popular performance metrics of distinguishing the near-field and far-field regions is known as the *Rayleigh distance*, which is given by $2D^2/\lambda$ [3]. Here, D and λ denote the RIS aperture and the wavelength, respectively. According to [4], the cascaded transmitter–RIS–receiver channel falls within the near-field region if either the transmitter–RIS distance or the RIS–receiver distance is shorter than the Rayleigh distance. Although near-field signal propagation is not a new phenomenon, due to the low operating frequencies and small antenna apertures employed in legacy wireless networks, the near-field coverage area has been negligible. Since the far-field region was dominant, planar wave-based far-field propagation has routinely been assumed for communication designs. However, when designing RISs for 6G, they will have a large aperture for realizing considerable array gains. They are eminently suitable for mm-wave/THz communications for circumventing their blockage issues [5]. Therefore, the near-field region in future RIS-aided communications becomes much larger and can no longer be ignored. For example, for a RIS with an aperture size of 1 m employed at the frequency of 28 GHz, the resultant Rayleigh distance is approximately 187 m.

Advantages of Near-Field Propagation for RISs

Given the above discussion, considering RIS-aided near-field communications is not a choice but a necessity. Compared to conventional RIS-aided far-field communications, the unique spherical wave-based near-field propagation leads to the following main advantages:

- *High-rank line-of-sight channels*: Recall that RISs are generally harnessed for circumventing the lack of line-of-sight (LOS) channels between transmitters and receivers. In RIS-aided far-field multiantenna/multiuser communications, the LOS channels usually exhibit a low rank; they may even have rank 1. This limits the achievable spatial multiplexing gains of RISs. By contrast, the near-field propagation channels tend to exhibit high rank, even potentially full rank, which provides enhanced DOF in RIS-aided near-field communications [4].

- *Precise near-field beam focusing capability*: In contrast to far-field beam steering, where the energy of wireless signals is concentrated to a specific angle, the spherical wavefront of RIS-aided near-field communications can be exploited to realize so-called beam focusing, where the energy of wireless signals is concentrated on a specific location at a given angle and distance. Given this new capability, the signal's energy in RIS-aided near-field communications can be more precisely delivered to the target receiver and prohibited from leaking to other receivers, thus achieving efficient multiuser communications in the vicinity of RISs [6].

Since the investigation of RIS-aided near-field communications is still in its infancy, its benefits have not been widely recognized. Hence, this article aims to provide a systematic easy-reading introduction to RIS-aided near-field communications, including near-field channel models, fundamental near-field performance analysis, near-field beam training, and near-field beamforming
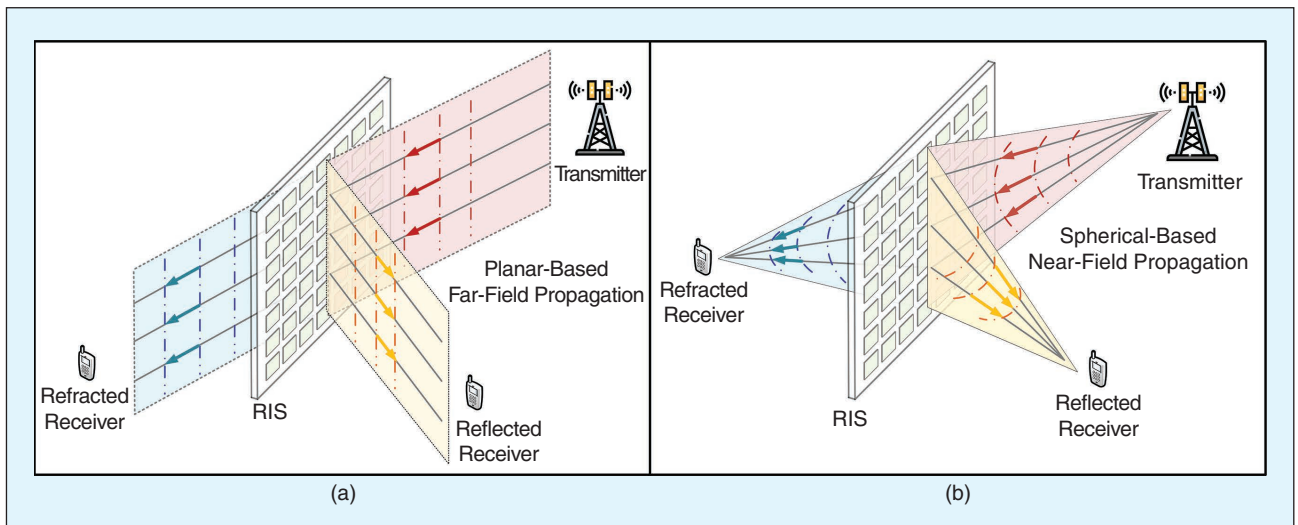

FIGURE 1 RIS-aided far-field and near-field communications, where the RIS can refract and/or reflect the incident signal to surrounding users. (a) Planar wave-based far-field propagation and (b) spherical wave-based near-field propagation.

design, complemented by a suite of future research challenges. The main contributions of this article can be summarized as follows:

- We classify RISs into two categories, namely, patch array-based RISs and metasurface-based RISs. For each type of RIS, we discuss key features, advantages, disadvantages, and near-field channel models.
- We characterize the fundamental performance limits of RIS-aided near-field communications, namely, power scaling laws and EDOF. We highlight RIS-aided near-field communications performance differences with regard to those in RIS-aided far-field communications.
- We discuss the associated beam training and beamforming design issues of RIS-aided near-field communications. In particular, a two-stage hierarchical beam training approach and an element-wise beamforming design are proposed, which significantly reduce the complexity of RIS-aided near-field communications.

Categories of RISs and Near-Field Channel Models

In this section, we first introduce the family of patch array-based and metasurface-based RISs. Then, we discuss their respective near-field channel models.

Patch Array- and Metasurface-Based RISs

Based on Figure 2, we introduce the key features, advantages, and disadvantages of these two types of RISs.

Patch Array-Based RISs

Again, RISs are composed of numerous low-cost elements capable of reconfiguring their phase-shift and amplitude responses. To mitigate their grating lobes, these elements are typically spaced at half-wavelength intervals. We refer to these conventional RISs as *patch array-based RISs*, as the phase-shift profile across the surface exhibits discontinuities. As illustrated in Figure 2(a), each element in the

patch array-based RIS possesses its own unique phase-shift response. The phase-shift coefficient remains constant within an individual element and independently changes among the elements. Patch array-based RISs are promising for employment at low frequencies, where the half-wavelength criterion suggests that the dimension of the elements is on the order of a few centimeters [7]. Therefore, a number of low-cost positive–intrinsic–negative diodes, varactor diodes, or delay lines can be installed at each element to realize high-resolution tunability. However, due to the short wavelength at high frequencies, the efficiency of patch array-based RISs diminishes; hence, their benefits might become marginal.

Metasurface-Based RISs

Metasurface-based RISs are realized using massive periodic cells with dimensions ranging from a few millimeters to micrometers or even to the molecular scale [7]. As described in Figure 2(b), metasurface-based RISs have the capability of quasi-continuous operation across the entire surface. Consequently, metasurface-based RISs require advanced control of the EM properties, including their conductivity and permittivity. Compared to patch array-based RISs, metasurface-based RISs are capable of operating at higher frequencies and exhibit beneficial phase-shift profiles, which leads to improved power scaling laws and EDOF (see the "Fundamental Performance Limits of RIS-Aided Near-Field Communications" section for details). However, the sophisticated control of metasurface-based RISs increases both their optimization and implementation complexity.

Near-Field Channel Models

Based on the above two types of RISs, we continue by introducing the representative near-field channel models for RIS-aided near-field communications.
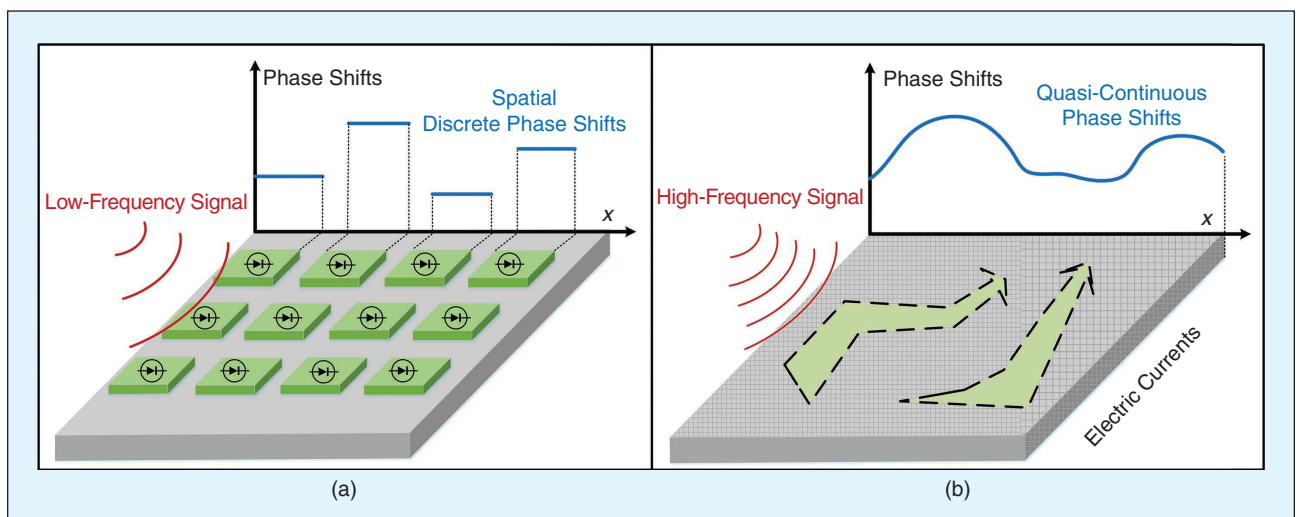

FIGURE 2 (a) Patch array-based RISs and (b) metasurface-based RISs.

Patch Array-Based RISs

For patch array-based RISs, the RIS-aided near-field MIMO channel can be accurately represented using a channel matrix having dimensions equal to the number of transmit and receive antennas. The entry (i, j) of the near-field channel is generally given by

$$[\mathbf{G}^{\text{LOS}}]_{i,j} = \sum_{m=1}^{M} \beta_{i,j,m} e^{-j\frac{2\pi}{\lambda}(\|\mathbf{r}_i - \mathbf{s}_m\| + \|\mathbf{s}_m - \mathbf{t}_j\|)} \qquad (1)$$

where $\beta_{i,j,m}$ denotes the distance-dependent path loss of a cascaded link; $\mathbf{s}_m$ is the Cartesian coordinate of the mth RIS element; $\mathbf{r}_i$ and $\mathbf{t}_j$ represent the Cartesian coordinates of the ith receive antenna and jth transmit antenna, respectively; and λ denotes the wavelength. Observe that the near-field channel model in (1) has nonuniform channel gains and nonlinear phases.

Metasurface-Based RISs

For metasurface-based RISs, the channel modeling process is more complex due to their quasi-continuous phase profile. Note that the key distinguishing feature of metasurface-based RISs is the presence of surface electric currents. To demonstrate this, we characterize the incident signal refracted/reflected by metasurface-based RISs to the receiver in the following three stages, with reference to Figure 3:

- *From incident signals to electric currents*: In the first stage, the RIS can be regarded as a source distribution system that produces a particular current density in space. When the wireless signals impinge upon the RIS, the incident EM field induces currents within the entire volume of the RIS.
- *From electric currents to scattered fields*: In the second stage, the time-varying electric currents radiate a controlled scattered field. We refer to the mapping from electric currents to the scattered field as *radiation*. Note that the process of radiation is the key factor determining the achievable DOF in the near field, which is discussed in the "EDOF" section.
- *From scattered fields to received signals*: In the third stage, the receiver can be regarded as a signal observation system, where the strengths of the received

electric field at different points on the aperture are calculated as a weighted sum.

In the first stage of metasurface-based RISs, continuous electric current distributions should be adopted for capturing the EM responses, instead of discrete phase-shift matrices. For the ideal scenario, where the receiver is completely accurate, the observation of the above third stage can be characterized by an identity matrix. In this case, the end-to-end channel gain between a transmitter and receiver associated with a RIS source current J is given by [7]

$$|h(J)|^2 = \frac{G A_T}{4\pi d^2} \int_{V_T} J^*(\mathbf{s}_1) \int_{V_T} K(\mathbf{s}_1, \mathbf{s}_2, \mathbf{r}) \, d\mathbf{s}_1 \, d\mathbf{s}_2 \qquad (2)$$

where G is the directivity of the transmit antenna, A_T is the aperture size of the RIS facing the transmitter, d is the distance between the transmitter and RIS, $\mathbf{s}_1$ and $\mathbf{s}_2$ are source points within the metasurface-based RIS, V_T denotes the volume of the metasurface-based RIS, $K(\mathbf{s}_1, \mathbf{s}_2, \mathbf{r})$ is the kernel function of the radiation operator, and $\mathbf{r}$ denotes the coordinates of the receiver. Note that the end-to-end near-field channel gain in (2) is subject to a given normalized source current distribution $J^*(\mathbf{s})$. In practice, the current distribution has to be optimized by harnessing specific near-field receivers.

Fundamental Performance Limits of RIS-Aided Near-Field Communications

Having highlighted the near-field channel models of RISs, in this section, we characterize the fundamental performance limits of RIS-aided near-field communications and discuss the performance differences both between the near-field and far-field regions as well as between both types of RISs.

Power Scaling Law

In the context of our discussion, the power scaling law is defined as the ratio between the received power P_r and transmit power P_t, which is a function of the RIS size. To study the power scaling differences between RIS-aided near-field communications and far-field communications, we consider a single-user system, where the RIS
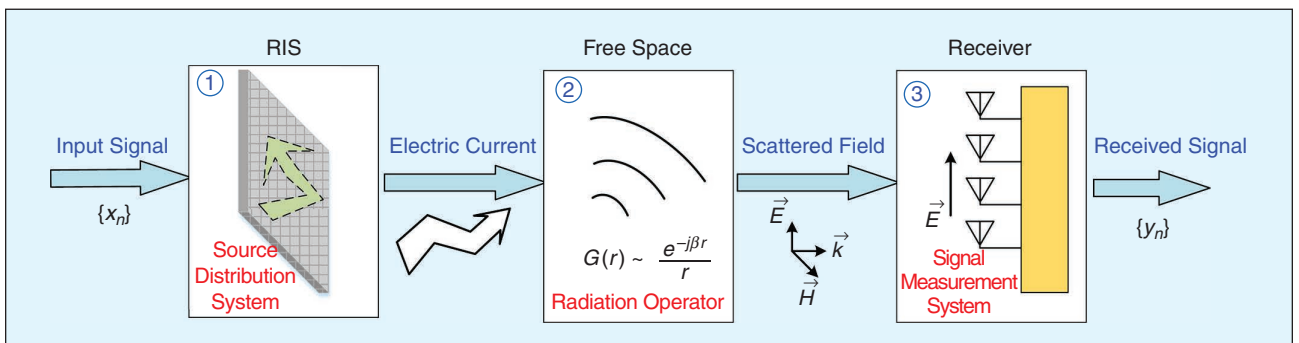

FIGURE 3 The three stages of a signal being refracted/reflected by a metasurface-based RIS to a receiver.

phase-shift coefficients are configured according to the cophasing condition for maximizing the end-to-end channel gain. We first discuss the different power scaling laws of RIS-aided near-field communications compared with those of RIS-aided far-field communications. Then, we discuss the power scaling law differences between patch array-based and metasurface-based RISs in near-field communications. In the following, we assume plane wave excitation. When the positions of the transmitter, RIS, and receiver are fixed, the received power is upper bounded by the transmit power, regardless of how large the RIS may become [8]. Thus, we consider near-field power scaling before this limit is reached.

RIS-Aided Far-Field Communications Versus Near-Field Communications

Observe in Figure 4 that conventional RIS-aided far-field communications exhibit quadratic power scaling. In particular, for patch array-based RISs, the received power scaling laws are proportional to the square of the number of RIS elements [2]. By contrast, for metasurface-based RISs, the received power scales with the square of the RIS aperture size [7]. However, for RIS-aided near-field communications, the received power scales linearly with the number of RIS elements or with the RIS aperture size. This is because within the near-field region, the

FIGURE 4 Power scaling laws for patch array-based and metasurface-based RISs. The receiver is located at a fixed distance of $d = 10$ m with respect to the center of the RIS, and the dimension of the receiver is $z_R \approx 5$ cm. The number of patch array-based RIS elements ranges from one to 20, and the aperture size of the metasurface-based RIS ranges from 1 to 4 cm^2. The wavelength of the carrier signal is 0.01 m.

subchannels associated with each of the RIS elements have different gains due to the varying path lengths. Therefore, the ratio of received power and transit power (P_r/P_t) of RIS-aided near-field communications scales slower than in RIS-aided far-field communications. To further illustrate this phenomenon, Figure 4 portrays P_r/P_t for both patch array-based and metasurface-based RISs, where the receiver has a fixed distance from the RIS. Observe in Figure 4 that as we increase the number of patch array-based RIS elements and the metasurface-based RIS aperture size, the near-field propagation becomes dominant, and the corresponding P_r/P_t scaling gradually changes from the rapid parabolic-shaped far-field quadratic scaling to the moderate linear near-field scaling.

Patch Array-Based RISs Versus Metasurface-Based RISs

For patch array-based and metasurface-based RIS-aided near-field communications, there is a slight difference in power scaling P_r/P_t. This is because for patch array-based RISs, each element is able to perform only a uniform phase-shift value over its cross section. By contrast, metasurface-based RISs facilitate more advanced control of the quasi-continuous phase-shift coefficients across the aperture. As a result, a higher normalized received power P_r/P_t can be achieved for metasurface-based RISs than for patch array-based RISs [7]. This is also confirmed by Figure 4, where the P_r/P_t slope of patch array-based RISs is less steep than that of metasurface-based RISs.

EDOF

The EDOF of a channel represent the number of independent parallel subchannels that can be supported. The achievable EDOF are determined by the hardware capabilities of the RIS and transceivers as well as the positioning of the receiver. In the following, we discuss and compare the EDOF of the RIS-to-receiver LOS MIMO channel in near-field communications and far-field communications, noting that the EDOF of the LOS multiantenna-transmitter-to-RIS channel can be characterized similarly. Generally speaking, the EDOF of the end-to-end RIS-aided channel are upper bounded by the minimum of the EDOF of the transmitter-to-RIS and RIS-to-receiver channels.

RIS-Aided Far-Field Communications Versus Near-Field Communications

For RIS-aided far-field communications, the EDOF of the RIS-to-receiver LOS MIMO channel is strictly equal to 1. By contrast, for RIS-aided near-field communications, the RIS-to-receiver LOS MIMO channel exhibits higher EDOF, which are generally larger than 1. This is because the varying path lengths associated with nonlinear phases allow the near-field channel to have a higher rank.
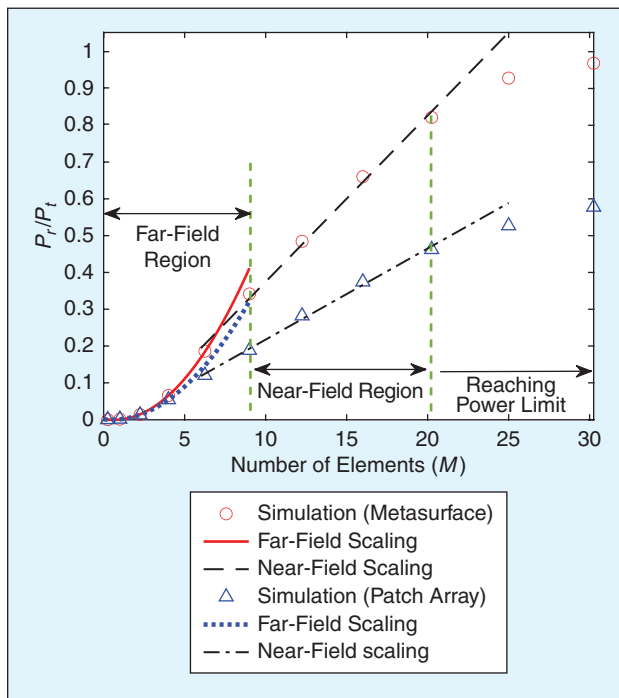
However, the near-field EDOF further depend on the shape, size, and geometric orientations of the transceivers. Nevertheless, [9] shows that the maximum numbers of EDOF between two rectangular prism volumes are roughly

$$N_{\max} = \frac{V_R V_T}{4(\lambda r)^2 \Delta z_T \Delta z_R} \qquad (3)$$

where $V_{R/T}$ are the volumes of the receiver/RIS, r is the distance, and $\Delta z_{R/T}$ are the width of the receiver/RIS. As we can see in this formula, the EDOF increase with the volumes and the decrease of distance r. As a result, as the receiver moves into the near-field regime of the RIS, the available EDOF may soon exceed the number of elements the patch array-based RIS may have. However, the metasurface-based RIS can fully exploit this $N_{\max}$. In the following, we provide a detailed discussion of the near-field EDOF for patch array-based and metasurface-based RISs.

Patch Array-Based RISs Versus Metasurface-Based RISs
For patch array-based RISs, the EDOF of the RIS–user channel is equal to its effective rank [10]. Consequently, the maximum achievable EDOF are limited by the number of RIS elements and the number of transceiver antennas. This implies that even when the near-field radiation operator exhibits higher EDOF, this cannot be achieved due to the hardware limitation of patch array-based RISs. However, for metasurface-based RISs, the near-field channel given in (2) is not restricted to a finite-dimensional matrix form. As a benefit, metasurface-based RIS-aided near-field communications generally have higher EDOF than the same-sized patch array-based RISs. To analytically derive the EDOF of the near-field channel for metasurface-based RISs, the EDOF of the scattered field (as demonstrated in Figure 3) have to be exploited [11]. For the scenario where the transceiver is equipped with a large number of antennas or a continuous-aperture antenna, there is no restriction on the EDOF of metasurface-based RISs, and the maximum EDOF determined by the near-field physical channel may indeed be achieved. Existing study [12] shows that the EDOF of a near-field channel is given by the number of large singular values of the radiation operator. For metasurface-based RISs, this number depends on the geometries of the RIS and receiver. For the case where the apertures of the RIS and

receiver are parallel to each other, the EDOF between a metasurface-based RIS and receiver are proportional to S/r^2, where S is the aperture size of the metasurface-based RIS and r is the communication distance [7].

The power scaling laws and EDOF of RIS-aided far-field communications and near-field communications are summarized and compared in Table 1. In general, metasurface-based RIS-aided near-field communications achieve better performance than patch array-based RIS-aided near-field communications.

Beam Training and Beamforming Design for RIS-Aided Near-Field Communications
Having discussed the fundamental performance limits of RIS-aided near-field communications, in this section, we discuss the specifics of efficient beam training and beamforming design of RIS-aided near-field communications.

Two-Stage Hierarchical Near-Field Beam Training

Overview of Near-Field Beam Training
The accurate acquisition of channel state information (CSI) is of vital importance for communication design. However, for RIS-aided near-field communications, CSI estimation becomes quite challenging. This is because having a large number of RIS elements and transceiver antennas leads to high-dimensional channels. The corresponding complexity of estimating the complete CSI may become excessive. Moreover, the passive nature of RISs makes the challenge graver. As a remedy, beam training is proposed. Relying on a predefined codebook consisting of different passive beamforming elements representing specific angular beams, beam training aims for determining the specific location of the target receiver both in terms of its angle and distance by selecting the optimal passive beamformer that achieves the maximum received signal power. By doing so, a high-quality initial link can be established for reduced-dimensional CSI estimation of the cascaded base station (BS)–RIS–user channel.

Although there are numerous research contributions on far-field beam training, they are unsuitable for near-field beam training. This may be explained from both a codebook design and training protocol perspective, as follows. The codebook design is the core of beam

TABLE 1 Performance differences between RIS-aided far-field communications and near-field communications.

Performance Metric	RIS-Aided Far-Field Communications	RIS-Aided Near-Field Communications	Patch Array-Based RIS-Aided Near-Field Communications	Metasurface-Based RIS-Aided Near-Field Communications
Power scaling law	Quadratic scaling	Linear scaling	Small scaling slope	High scaling slope
Transmitter/Receiver–RIS LOS MIMO channel EDOF	Strictly equal to 1	Usually larger than 1	Limited by element/antenna number	Not limited

training, which directly determines the ultimate accuracy. Upon recalling that the near-field channels require both angular and distance information, the angle-only codebooks developed for far-field beam training become inefficient due to the energy spread effect [13, Sec. IV-A]. Explicitly, the energy of a far-field beamformer designed for a specific angle will spread to a range of different angles in the near field. As a result, the accuracy of the beamformer becomes gravely degraded. Circumventing this requires a codebook tailored to near-field beam training, where the codebook has to cater to both the discrete angular domain and the discrete distance domain, i.e., in the polar domain. Hence, compared to the far-field codebook, the near-field codebook becomes much larger, which further increases the complexity of near-field beam training. This calls for efficient near-field training protocols to be developed.

Proposed Beam Training Approach

Given the above challenges, a novel two-stage hierarchical beam training approach was proposed in [13], which can be harnessed for RIS-aided near-field communications. As shown in Figure 5, the BS and RIS usually have fixed locations and thus have a LOS link between them. The corresponding BS–RIS channel is typically quasi-static in practice. The main challenge lies in the beam training of the RIS user near-field transmitting/reflecting channel. To address this issue, based on the BS–RIS channel obtained, the BS's transmit beamforming can be directed toward the RIS. Then, the cascaded BS–RIS–user near-field beam training can be reduced to the RIS–user near-field beam training relying on the proposed two-stage hierarchical beam training approach. In the following, we provide a brief introduction to the proposed beam training approach.

To mitigate the above-mentioned near-field energy spread effect, the proposed approach relies on initially activating a small central subarray of the entire array during the beam training. The key idea is that upon activating a small subarray, far-field propagation becomes dominant, and the near-field energy spread effect is reduced. Motivated by this observation, as detailed in Figure 6, two stages are involved in the proposed approach, namely, the coarse angular estimation stage of far-field communications and the joint angular and distance estimation stage. The number of layers in stage 1 and stage 2 are denoted by L_1 and L_2, respectively. With the gradual increase of the number of layers, the number of activated RIS elements also increases until all the elements become activated in the last layer. The total number of layers, $L_t = L_1 + L_2$, is determined by the total number of RIS elements denoted by N; i.e., $L_t = \log_2(N)$. For each stage, the main procedure may be formulated as follows:

- *Stage 1—coarse angular estimation*: As shown in Figure 6(a), each layer activates only a relatively small number of RIS elements. In this case, users can be regarded as located in the far-field region of the RIS, where the near-field energy spread effect is negligible. Therefore, the conventional hierarchical far-field codebook that distinguishes only the angular domain is employed for coarsely estimating a user's angular information.
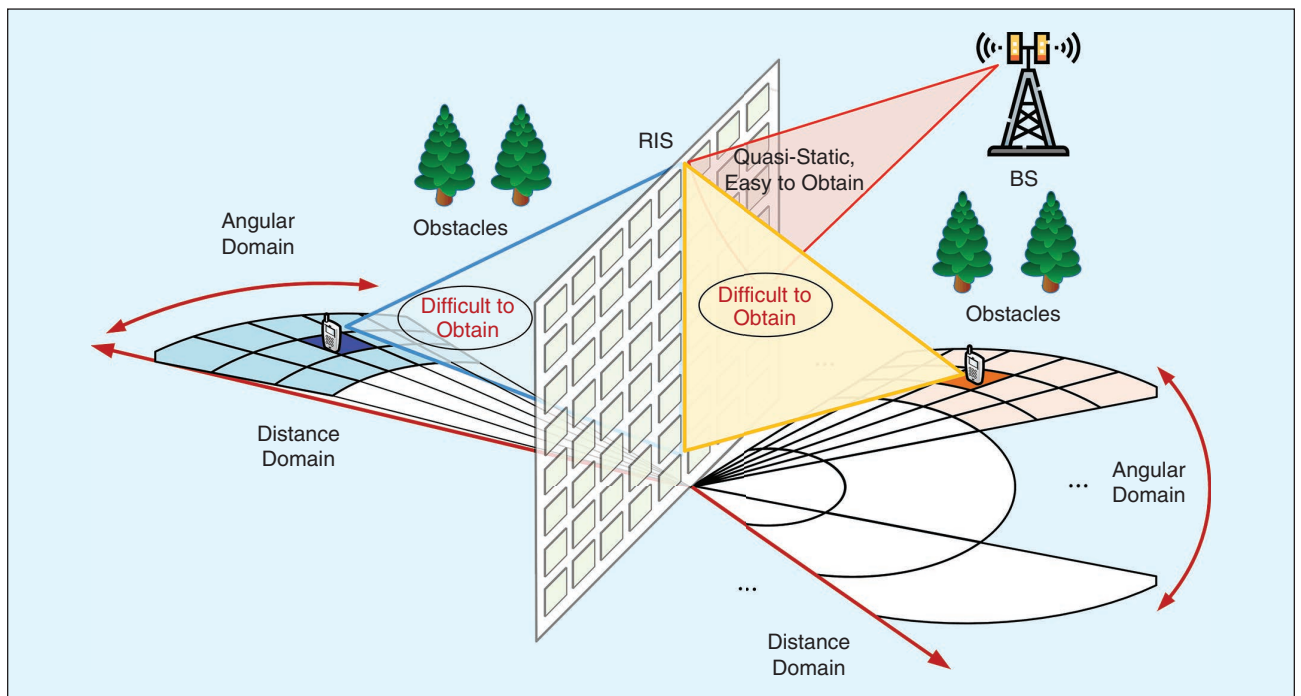

FIGURE 5 The beam training in RIS-aided near-field communications.

■ *Stage 2—joint angular and distance estimation*: As apparent in Figure 6(b), given a reduced user angle candidate set estimated by stage 1, this stage further increases the number of activated RIS elements; hence, near-field propagation becomes dominant. This stage then employs an appropriately designed hierarchical polar domain codebook for jointly estimating the user's angular and distance information. In particular, each codeword within the hierarchical polar domain codebook corresponds to a distinct combination of a sampled angular direction and sampled distance. The design of hierarchical polar domain codebooks follows two criteria: 1) in each layer, the entire angular and distance domains (i.e., the polar domain) are comprehensively represented by all the codewords, and 2) the polar domain of a codeword within a particular layer should encompass the union of polar domains represented by several codewords in the subsequent layer.

The main advantage of the proposed two-stage hierarchical beam training technique is that the training overhead can be significantly reduced. It was shown in [13] that the training overhead in the proposed approach [on the order of $O(\log_2(N))$] reduces to 1% and 5% of that in the exhaustive search-based near-field beam training [on the order of $O(NS)$] and two-phase beam training of [14] [on the order of $O(N+S)$], respectively, where S denotes the number of sampled distances. Note that there is a tradeoff between the training overhead and achievable performance in the proposed two-stage hierarchical beam training approach for different L_1 and L_2. Due to the employment of the polar domain codebook, each layer in stage 2 can achieve a higher accuracy but consumes a higher training overhead than that in stage 1 using the angular domain codebook. Therefore, L_1 and L_2 should be carefully selected to strike a good tradeoff selection. Detailed discussions of selecting L_1 and L_2 can be found in [13, Sec. IV-B].

Low-Complexity Element-Wise Near-Field Beamforming Design

Efficient beamforming design is critical for creating a "smart radio environment" by RISs and, thus, for improving the overall communication performance. For
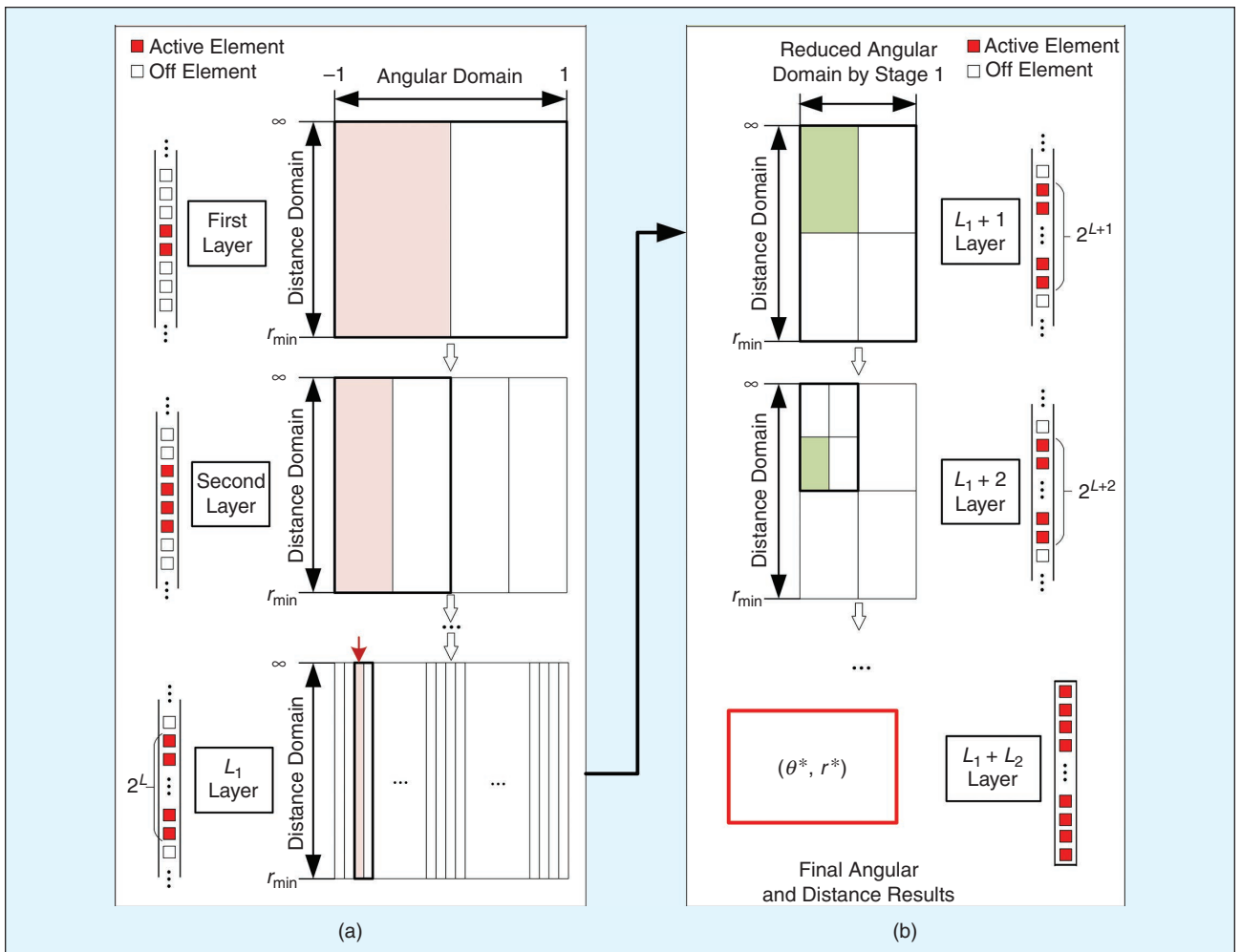

FIGURE 6 The proposed two-stage hierarchical beam training approach with the subarray technique. More technical details can be found in [13]. (a) Stage 1: coarse angular estimation. (b) Stage 2: joint angular and distance estimation.

RIS-aided near-field communications, an intrinsic feature is that the total number of RIS elements is generally large, which leads to potentially high computational complexity. Therefore, the existing beamforming methods proposed for RIS-aided far-field communications might be unsuitable for deriving high-dimensional near-field beamforming solutions. To address this issue, a novel element-wise optimization framework was proposed for simultaneously transmitting and reflecting (STAR)–RIS-aided near-field communications in [15]. For STAR–RIS having N elements, the key idea is that only a single specific STAR–RIS coefficient is optimized at a time, with all the other $N-1$ coefficients fixed. Each element-wise STAR–RIS coefficient optimization problem is convex and easy to solve. Therefore, the resultant computational complexity increases only linearly with the number of STAR–RIS elements, i.e., on the order of $O(N)$, compared to that of the conventional beamforming method, on the order of $O(N^3)$. This is attractive for practical implementations. In [15], it was shown that the computational time of the proposed element-wise approach required for optimizing the entire STAR–RIS beamforming vector in each iteration is merely 0.04% of that of the conventional optimization approach. The performance gap in terms of the weighted sum rate between the proposed approach and conventional optimization approach is less than 5%.

To further illustrate the benefits of RIS-aided near-field communications, Figure 7 compares the performance of STAR–RIS-aided multiuser MIMO communication in near-field and far-field propagations [15]. Observe that near-field pr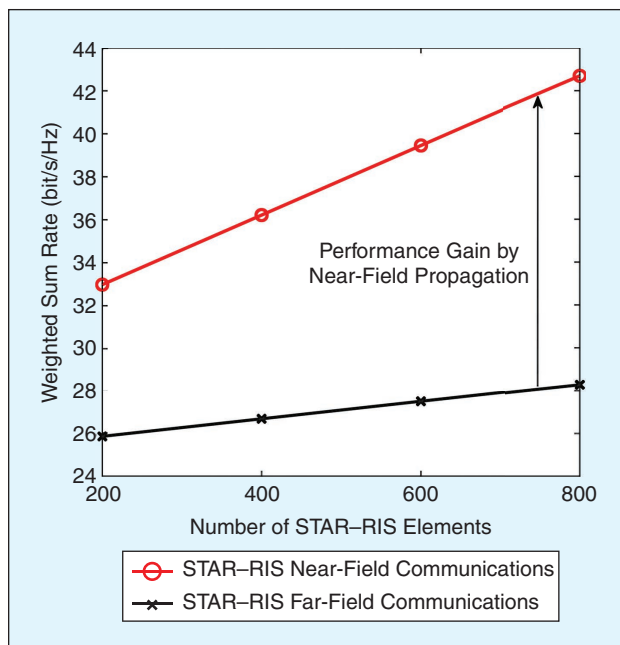opagation attains a higher weighted sum rate than far-field propagation. This is because the high-rank LOS channel and near-field beam focusing capability further mitigate the multiuser interference and thus improve the data rate. Moreover, it can be found that the rate enhancement attained by increasing the number of STAR–RIS elements is more pronounced in the near field than in the far field. This also underscores the benefits of RIS-aided near-field communications.

Conclusions and Research Opportunities

In this article, RIS-aided near-field communications have been discussed for future 6G wireless networks. In particular, both patch array-based and metasurface-based RISs were discussed, and corresponding near-field channel models were introduced. Based on the near-field channel models, the power scaling law and EDOF were analyzed, which were compared to those of RIS-aided far-field communications. Furthermore, the beam training and beamforming design of RIS-aided near-field communications were discussed. A two-stage hierarchical near-field beam training approach was proposed, which is capable of significantly reducing the training overhead. An element-wise beamforming design method was developed for obtaining the high-dimensional beamforming coefficients at a low computational complexity. Note that the design of RIS-aided near-field communications still has many research challenges, some of which are discussed as follows:

- *Near-field CSI estimation, beam training, and beamforming design for metasurface-based RISs*: While metasurface-based RISs hold significant promise for performance enhancement in near-field communications, the intricate nature of the Green's function-based near-field channel model and the quasi-continuous configuration introduce more design challenges compared to patch array-based RISs. Further research efforts, involving advanced theories and mathematical tools, are required to fill the knowledge gap.

- *Dynamic RIS configuration for adjustable near-field and far-field regions*: Since the Rayleigh distance depends on the RIS aperture size, adjustable near-field and far-field regions can be facilitated by switching specific RIS elements on and off, i.e., modifying the aperture size. Note that although higher DOF and capacity enhancements can be achieved in the near-field region, the complexity of determining the CSI and beamforming design significantly increases. By exploiting the adjustable near-field and far-field regions provided by the dynamic RIS configuration, an appealing tradeoff can be struck between the performance achieved and complexity imposed. This constitutes an interesting future research topic.

- *Exploiting generative artificial intelligence in RIS-aided near-field communications*: Generative artificial intelligence (GAI) techniques have demonstrated substantial potential in the field of wireless communications. To address the complex optimization challenges

FIGURE 7 The achieved weighted sum rate versus the number of STAR–RIS elements in near-field communications and far-field communications. The system parameters can be found in [15].

associated with near-field channels and the vast number of optimization variables in RIS-aided near-field communications, GAI techniques, such as generative adversarial networks, transformers, and diffusion models, are emerging as promising solutions. For instance, their generative capabilities can be harnessed to create suitable codebooks and efficient beam search strategies during near-field beam training as well as to facilitate near-field beamforming design and resource management in the presence of CSI uncertainties. These applications require further investigation.

Acknowledgment

Author Information
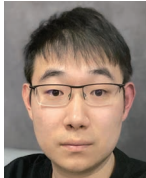
Xidong Mu (xidong.mu@qmul.ac.uk) is currently a postdoctoral researcher with the School of Electronic Engineering and Computer Science, Queen Mary University of London, E1 4NS London, U.K. He received the 2023 IEEE Communications Society Outstanding Young Researcher Award for the Europe, Middle East, and Africa region and the 2022 International Symposium on Wireless Communication Systems Best Paper Award, among others. He is a Member of IEEE.

Jiaqi Xu (jiaqi.xu@qmul.ac.uk) is currently a postdoctoral research associate at University of California, Irvine, CA 92697 USA. He received the B.S. degree in physics and computer science from Peking University, China, and the Ph.D. degree in electrical engineering from Queen Mary University of London, U.K. His research interests mainly focus on the intersection of physics, wireless communication, and computing. He is a Member of IEEE.

Yuanwei Liu (yuanwei.liu@qmul.ac.uk) is a senior lecturer at Queen Mary University of London, E1 4NS London, U.K. His research interests include reconfigurable intelligent surfaces/simultaneously transmitting and reflecting, near-field communications, and machine learning. He is an IEEE Communications Society Distinguished Lecturer and an IEEE Vehicular Technology Society Distinguished Lecturer. He also serves as an area editor of *IEEE Communications Letters* and an editor of *IEEE Transactions on Vehicular Technology*. He is a Fellow of IEEE.

Lajos Hanzo (lh@ecs.soton.ac.uk) is with the School of Electronics and Computer Science, University of Southampton, SO17 1BJ Southampton, U.K., where he holds the chair in telecommunications. He received the Ph.D. degree in electronics in 1983. He has successfully supervised 120-plus Ph.D. students; coauthored 19 Wiley/IEEE Press books on mobile radio communications, totaling more than 10,000 pages; and published 2,000+ research contributions on IEEE *Xplore*. He is a Life Fellow of IEEE.

References

[1] C.-X. Wang et al., "On the road to 6G: Visions, requirements, key technologies, and testbeds," *IEEE Commun. Surveys Tuts.*, vol. 25, no. 2, pp. 905–974, Second Quart. 2023, doi: 10.1109/COMST.2023.3249835.

[2] M. Di Renzo et al., "Smart radio environments empowered by reconfigurable intelligent surfaces: How it works, state of research, and the road ahead," *IEEE J. Sel. Areas Commun.*, vol. 38, no. 11, pp. 2450–2525, Nov. 2020, doi: 10.1109/JSAC.2020.3007211.

[3] J. D. Kraus and R. J. Marhefka, *Antennas for All Applications*. New York, NY, USA: McGraw-Hil.

[4] M. Cui et al., "Near-field MIMO communications for 6G: Fundamentals, challenges, potentials, and future directions," *IEEE Commun. Mag.*, vol. 61, no. 1, pp. 40–46, Jan. 2023, doi: 10.1109/MCOM.004.2200136.

[5] H. Zhang et al., "6G wireless communications: From far-field beam steering to near-field beam focusing," *IEEE Commun. Mag.*, vol. 61, no. 4, pp. 72–77, Apr. 2023, doi: 10.1109/MCOM.001.2200259.

[6] H. Zhang et al., "Beam focusing for near-field multiuser MIMO communications," *IEEE Trans. Wireless Commun.*, vol. 21, no. 9, pp. 7476–7490, Sep. 2022, doi: 10.1109/TWC.2022.3158894.

[7] J. Xu et al., "Exploiting STAR-RISs in near-field communications," *IEEE Trans. Wireless Commun.*, early access, doi: 10.1109/TWC.2023.3296191.

[8] E. Björnson and L. Sanguinetti, "Power scaling laws and near-field behaviors of massive MIMO and intelligent reflecting surfaces," *IEEE Open J. Commun. Soc.*, vol. 1, pp. 1306–1324, 2020, doi: 10.1109/OJCOMS.2020.3020925.

[9] D. A. Miller, "Communicating with waves between volumes: Evaluating orthogonal spatial channels and limits on coupling strengths," *Appl. Opt.*, vol. 39, no. 11, pp. 1681–1699, 2000, doi: 10.1364/AO.39.001681.

[10] O. Roy and M. Vetterli, "The effective rank: A measure of effective dimensionality," in *Proc. 15th Eur. Signal Process. Conf.*, Poznan, Poland, 2007, pp. 606–610.

[11] O. M. Bucci and G. Franceschetti, "On the degrees of freedom of scattered fields," *IEEE Trans. Antennas Propag.*, vol. 37, no. 7, pp. 918–926, Jul. 1989, doi: 10.1109/8.29386.

[12] M. Migliore, "On the role of the number of degrees of freedom of the field in MIMO channels," *IEEE Trans. Antennas Propag.*, vol. 54, no. 2, pp. 620–628, Feb. 2006, doi: 10.1109/TAP.2005.863108.

[13] C. Wu et al., "Two-stage hierarchical beam training for near-field communications," *IEEE Trans. Veh. Technol.*, early access, 2023, doi: 10.1109/TVT.2023.3311868.

[14] Y. Zhang et al., "Fast near-field beam training for extremely large-scale array," *IEEE Wireless Commun. Lett.*, vol. 11, no. 12, pp. 2625–2629, Dec. 2022, doi: 10.1109/LWC.2022.3212344.

[15] H. Li et al., "Near-field beamforming for STAR-RIS networks," 2023, *arXiv:2306.14587*.

VT